Surface Modification of MgO Microcrystals by Cycles of Hydration-Dehydration

Hae-Jin Kim, Jin Kang, Me Young Song, Seon Hui Park, Dong Gon Park,* Ho-Jin Kweon,† and Sang Sung Nam‡

Department of Chemistry, Sookmyung Women's University, Seoul 140-742, Korea
†Samsung Display Devices Co., Ltd., Chunan 330-300, Korea
‡Korea Research Institute of Chemical Technology, Taejon 305-600, Korea
Received May 26, 1999

Relatively inert surface of microcrystalline MgO was modified into chemically active one by carrying out controlled hydration followed by dehydration at elevated temperature under dynamic vacuum. Even though the treatment by the first cycle of hydration-dehydration did not alter the porosity of MgO, it largely enhanced surface reactivity of the MgO toward adsorbed water, turning its outer layer into brucite upon rehydration. Treatment by the second cycle of hydration-dehydration generated micropores, and slit-shaped mesopores, raising the porosity of the MgO. The overlayer of Fe_2O_3 of the core/shell type composite magnesium oxide enhanced this surface modification, turning its surface into more porous and more active one than that of uncoated MgO, after the treatment by the hydration-dehydration.

Introduction

In many natural phenomena and technological applications, surfaces of metal oxides take an extremely important role. Fundamental understanding of the oxide surfaces is necessary to fully describe many processes, such as catalysis and corrosion.[1] Especially, the reaction between water and oxide surfaces takes central role in many geological processes, such as soil degradation, weathering, and sedimentation.

Having very simple crystal structure of rock salt, magnesium oxide, MgO, has been extensively studied as a model system for the surfaces of ionic solids. Compared to other metal oxides, there are more theoretical studies carried out on the MgO surfaces.[2-8] In carrying out theoretical calculations, main interest was usually on (100) surface, which was considered to be the most stable crystalline surface of MgO. Discrepancy among experimental observations and theoretical calculations have attracted much curiosity on the surface property of MgO.[1,5] Especially, the reactivity of MgO toward adsorbed chemicals was observed to depend strongly on how the sample was prepared.[9-11] Whereas, polycrystalline powder of MgO exhibited high reactivity toward various small molecules, theoretical calculation indicated that the reaction of small molecules with (100) facet was energetically unfavorable.[3] It predicted that reaction between water and clean (100) surface should be physisorption rather than chemisorption, which contradicted several experimental outcomes. Explanation was sought from surface defects which provide active sites,[5] such as corners, edges, steps, and kinks, and different crystallographic facets, especially (111) facet. It was experimentally observed that (111) surface of MgO exhibited high reactivity toward various chemicals.[11]

Depending on preparation method, MgO exhibited quite different reactivity toward adsorbed chemicals. For example, organophosphorous compounds decomposed more readily on nanocrystalline MgO than on microcrystalline MgO, which were prepared via very different synthetic routes.[12-14] Halogenated carbons also decomposed readily on nanocrystalline MgO. If a layer of Fe_2O_3 was applied on MgO, thereby, forming core/shell type composite metal oxide, the reaction between MgO and CCl_4 was greatly enhanced, and became almost stoichiometric when the core was nanocrystalline.[15-17] Plausible explanation for the observed enhancement of the reaction between MgO and CCl_4 was suggested in our previous report.[18]

In many aspects, those different MgO samples exhibited quite different surface chemistry. It was observed that surface property of MgO could be altered in significant extent simply by carrying out hydration and dehydration on the surface of MgO.[15-18] Depending on the extent of the hydration, subsequent dehydration brought about very different outcome. In this report, surface modification of microcrystalline MgO by cycles of hydration and dehydration was reported for the case where the least amount of initial hydration was allowed. The case where the initial hydration was maximized by direct contact with liquid water will be dealt in other report which should follow this one.

Experimentals

Calcined magnesia (MgO) powder was purchased from Fisher Scientific. Hydration of the surface was carried out by exposing the powder to 100% relative humidity (RH) for several days. A few grams of the hydrated powder was charged in a 100 mL Schlenk reaction vessel (SRV), and carefully heated up to 500 °C (around 50 °C per hour), and left at the temperature for overnight under dynamic vacuum of around 10^{-3} torr. This processing will be designated as the first cycle of hydration-dehydration. After the powder was cooled down to room temperature, it was kept under argon. The MgO powder obtained as above corresponds to the one

*To whom correspondence should be addressed.

designated as CM-MgO in previous study.[18] A fraction of the CM-MgO was transferred into an open container, and kept under 100% RH for sufficient period (20-40 days) in order to fully rehydrate the surface. The hydrated powder was heated at 300 °C for 10h under dynamic vacuum. It was known that bulk transition from $Mg(OH)_2$ to MgO was completed at 300 °C.[19] This processing will be designated as the second cycle of hydration-dehydration.

The core/shell type composite oxide of $[Fe_2O_3]$CM-MgO was synthesized by putting an overlayer of Fe_2O_3 over the CM-MgO as described in the previous report.[18] The hydration-dehydration treatment was carried out with the core/shell type composite oxide, too.

Powder X-ray diffraction (PXRD) patterns were taken from the MgO samples by using Scintag PAD-X diffractometer. FTIR spectra were taken by Nicolet Impact-400, from the samples which were made into pellets with KBr. Surface image of CM-MgO prior to the second cycle treatment was obtained by atomic force microscope (AFM) using Scanning Probe Microscope (SPM) M-30 (Wyco), from a pellet made by pressing 0.1 g of the powder at 11,000 psi. Nitrogen adsorption-desorption characteristics were measured by using ASPS-2400 Micromeritics. Care was taken so that the exposure of the samples to humidity was minimized. BET surface area and pore size distribution were obtained from the nitrogen adsorption-desorption isotherm.[20] Characterization of microporosity of the samples was carried out by obtaining t-plots from the isotherms.[20,21]

Results and Discussion

Surface feature of the pellet pressed from CM-MgO powder was shown in Figure 1. AFM image of CM-MgO showed a collection of aligned particles in a plate-like shape of around 200 nm wide and 50 nm thick. It was presumed that the alignment was caused by pellet pressing.[18] The overall feature of the particles was not much different from the core/shell type composite magnesium oxide, $[Fe_2O_3]$CM-MgO, whose AFM image was reported previously.[18] The surface of the platelets was very flat and smooth. Taking the image with a same force on the probe, it appeared that the surface of $[Fe_2O_3]$CM-MgO was rougher than that of CM-MgO.[18] This plate-like shape with smooth flat surface suggested that the surface of CM-MgO was composed predominantly of (100) crystallographic facet.[22]

The FTIR spectra taken from the MgO samples were provided in Figure 2. The spectrum (Figure 2A) taken from commercially purchased magnesia which was exposed to 100% RH for several days had peaks around 3500 cm^{-1} and 1500-1600 cm^{-1} for the physisorbed water on the oxide surface. The vibrations were very broad due to hydrogen bonding interaction. After the first cycle, overall pattern of the spectrum was not much changed. Isolated hydroxyls were not observed (Figure 2B and 2C). This observation indicated that the extent of bulk hydroxylation by adsorbed water was not that significant. Bulk hydroxylation was not observed in the MgO as purchased. Therefore, the integrity of the MgO microcrystallites was mostly preserved during the first cycle, which conformed to the AFM observation of platelets with flat surfaces. When CM-MgO was exposed again to 100% RH, a sharp peak developed at 3700 cm^{-1} (Figure 2D). The peak was very sharp, which indicated the hydroxides on the surface were isolated ones without mutual hydrogen bonding interaction. Those peaks at 3700, 3650, 3400 cm^{-1} coincided with the ones reported for nominal surface of brucite ($Mg(OH)_2$) crystal.[23] The broad peak of the chemisorbed

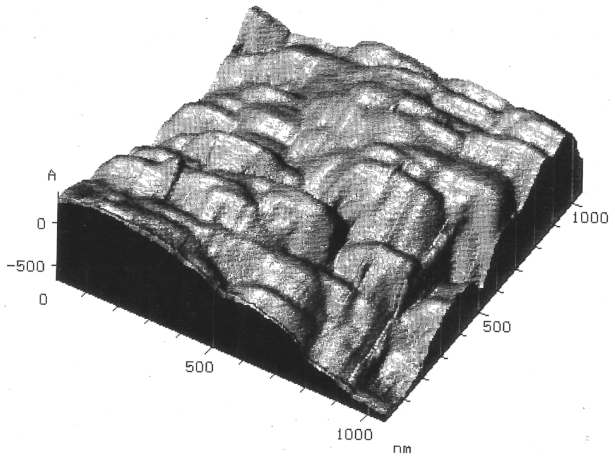

Figure 1. AFM micrograph of a pellet made by pressing CM-MgO powder, before it was exposed to humidity for the second cycle treatment.

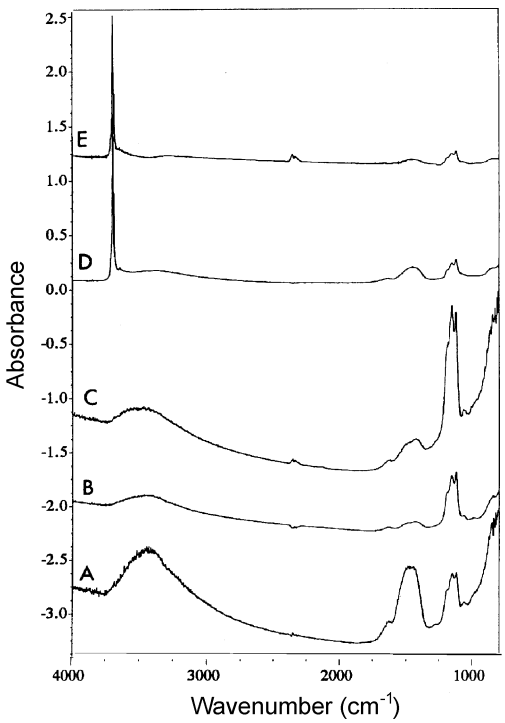

Figure 2. FTIR spectra taken from MgO samples. Spectrum (A) is the one obtained from commercial MgO exposed to humidity. Spectrum (B) is from CM-MgO, and (C) is from $[Fe_2O_3]$CM-MgO, both before being exposed to humidity for the second hydration. Spectrum (D) is from CM-MgO, and (E) is from $[Fe_2O_3]$CM-MgO, both after they were hydrated for the second cycle treatment.

water around 3500 cm^{-1} was nearly absent. Therefore, the outer layer of the CM-MgO was all transformed into the brucite. The spectral change observed for $[Fe_2O_3]$CM-MgO followed the same track as the CM-MgO, except the fact that the broad peak around 3400 cm^{-1} was shifted to 3300 cm^{-1}. It was speculated that the existence of iron on the surface caused the spectral shift.

The observation of only the sharp hydroxide vibration indicated that the surface hydroxylation progressed in large extent, down into the bulk. Considering such deep hydroxylation was not occurred in the MgO as purchased, the first cycle of hydration-dehydration apparently generated active sites on the surface of CM-MgO. Theoretical calculation suggested water molecules chemisorbed on low-coordinated magnesium in those defective sites,[5] whereas they physisorbed on the perfect (100) surface.[3] Therefore, the flat (100) surface which was relatively inert toward chemisorption turned into highly defective surface which should be more prone to the chemisorption. Those active sites,[5,8] such as edges, kinks, corners, steps, and (111) planes exposed,[11] must have provided sites for chemisorption by water, which eventually lead to the bulk hydroxylation.

In order to assess the extent of the bulk hydroxylation, PXRD patterns were taken from CM-MgO and $[Fe_2O_3]$CM-MgO, before and after the second hydration. In both samples, diffraction peaks of brucite were observed after the second hydration in 100% RH. Because diffraction is bulk

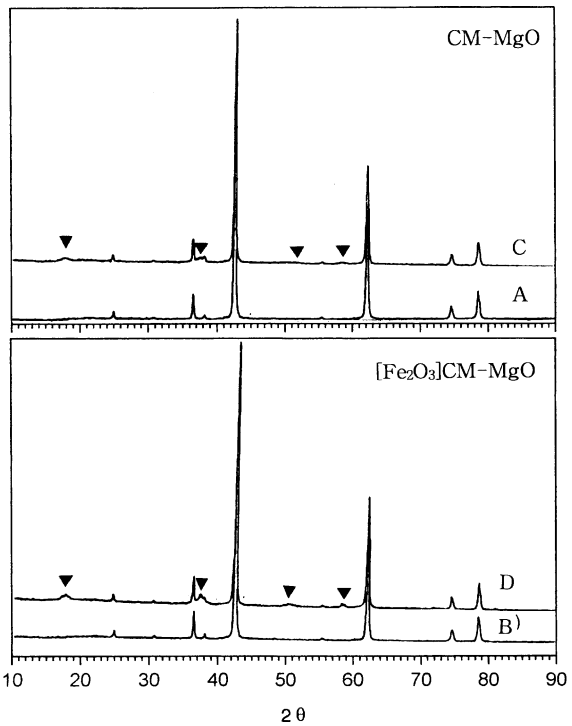

Figure 3. Powder X-ray diffraction patterns of the MgO samples. Patterns (A) and (B) are the ones obtained before the samples were exposed to humidity for the second cycle treatment. Patterns (C) and (D) are the ones obtained from the hydrated samples before they were dehydrated for the second cycle treatment. Closed triangles designate diffractions from outer layers of brucite, $Mg(OH)_2$.

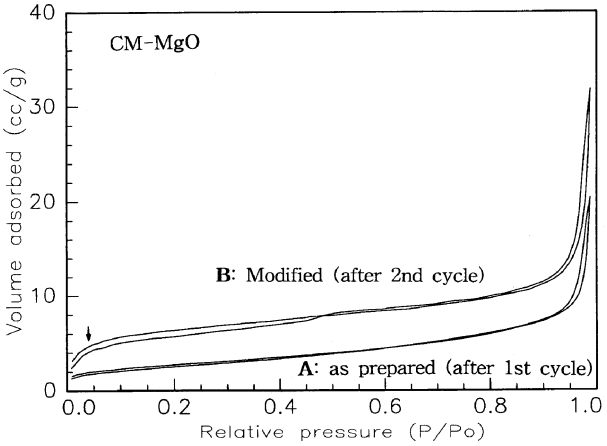

Figure 4. Isotherms of nitrogen adsorption-desorption on the surface of microcrystalline MgO, (A) after the first cycle treatment which produced the CM-MgO, and (B) after the second cycle treatment which produced modified CM-MgO. A small arrow points at the inflection point raised.

property, the observation of those brucite peaks suggests that surface hydroxylation proceeded deep into the bulk, converting several outer layers of MgO into $Mg(OH)_2$, brucite. By assessing from relative intensity of the peaks, more MgO was converted to $Mg(OH)_2$ in $[Fe_2O_3]$CM-MgO than in CM-MgO. If only the surface area was the factor to influence the extent of hydroxylation, the opposite should be observed, because surface area of $[Fe_2O_3]$CM-MgO was smaller than CM-MgO (see Table 1 below). Considering (100) surface of MgO was inactive toward chemisorption (conversion of MgO to $Mg(OH)_2$),[3] it was presumed that the surface of $[Fe_2O_3]$CM-MgO should contain more active sites (defects) than that of CM-MgO. In previous report, it was observed that initial reactivity of CM-MgO toward CCl_4 was largely increased by the overcoat of Fe_2O_3 layer,[18] which corroborated this suggestion. The above AFM observation, which showed that the surface of $[Fe_2O_3]$CM-MgO was rougher than that of CM-MgO, corroborated this reasoning, too.

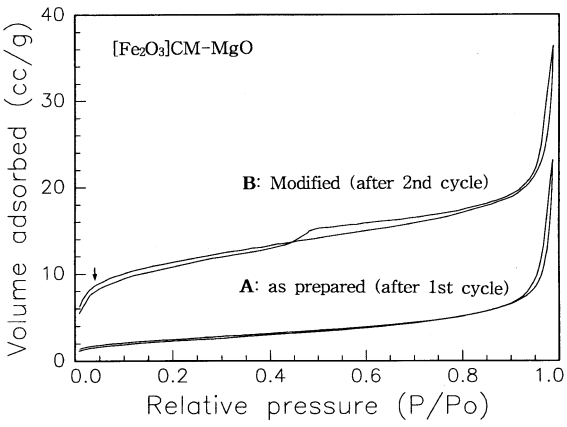

Figure 5. Isotherms of nitrogen adsorption-desorption on the surface of core/shell type composite magnesium oxide, (A) after the first cycle treatment which produced the $[Fe_2O_3]$CM-MgO, and (B) after the second treatment which produced modified $[Fe_2O_3]$CM-MgO.

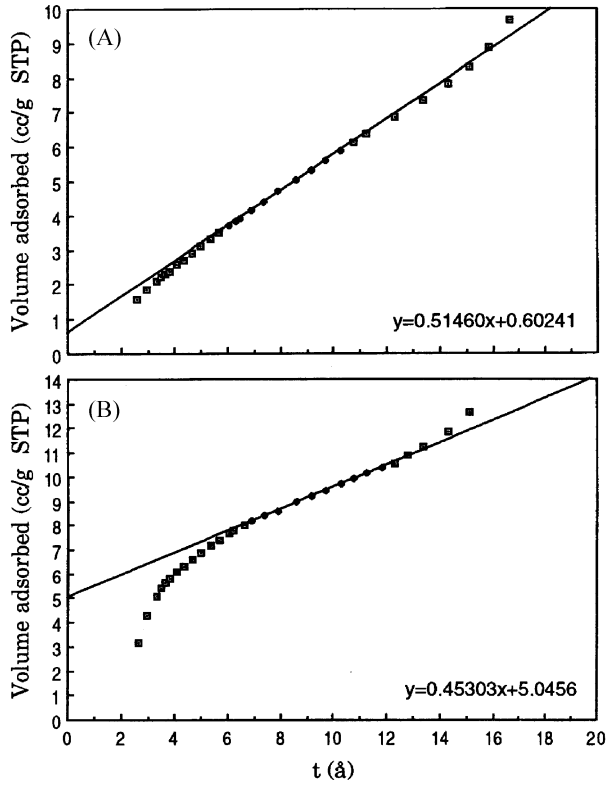

Figure 6. A t-plot calculated from the isotherm obtained from CM-MgO before the second cycle treatment (A). After the second cycle treatment, the t-plot (B) showed that surface characteristics were largely modified.

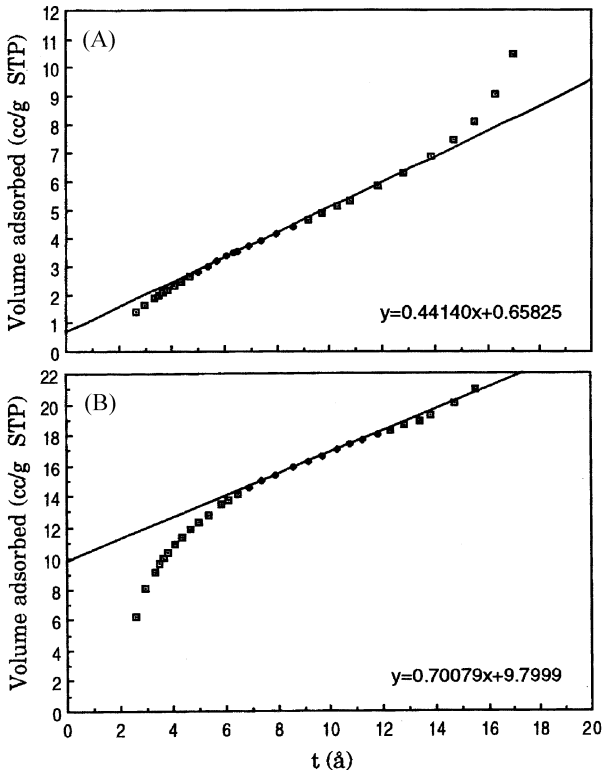

Figure 7. T-plots calculated from the isotherms obtained from $[Fe_2O_3]$CM-MgO, (A) before the second cycle treatment, and (B) after the treatment.

Pore characteristics of solid samples can be glimpsed by observing the adsorption-desorption behavior of nitrogen on the surface of the samples. Figure 4 and 5 showed the isotherms of the adsorption-desorption of nitrogen on the surface of CM-MgO and $[Fe_2O_3]$CM-MgO, before (after the completion of the first cycle) and after the second cycle of hydration-dehydration. The isotherms before the second cycle were type II and exhibited almost no hysteresis. These features are typical characteristics of non-porous solids.[20] Total surface area (S_{total}) was calculated by BET method,[20] and provided in Table 1. As can be anticipated, they had relatively small BET surface area, 9.8 and 9.0 m^2/g. From the isotherms, t-plots were derived,[20,21] and were provided in Figure 6 and 7. Before the second cycle, the fitted line extrapolated near to origin (Figure 6A and 7A), which confirmed that those samples were non-porous, not having much micropores. By using the total surface area and the slope of the fitted line, surface area generated by micropores (S_{micro}) was calculated, and provided in Table 1. The surface area generated by micropores was only 24 and 19% in $[Fe_2O_3]$CM-MgO and CM-MgO, respectively.

The isotherms after the second cycle also had shape of type II. But, considering the first inflection point was raised (Figure 6B and 7B), it was suggested that fair amount of micropores were generated during the second cycle treatment. Supporting this, the fitted lines of the t-plots after the second cycle passed through positive intercepts. The studies on the decomposition of brucite at high temperature showed that $Mg(OH)_2$ transformed into a collection of perfect nanocubes of MgO upon decomposition.[24-26] It was suggested that those cubes faced each other, forming microslits, which necessarily increased surface area of the sample. Therefore, during the second cycle treatment, the micropores were generated as the outer layer of $Mg(OH)_2$ was transformed into MgO cubes upon dehydration. The inflection point was higher in $[Fe_2O_3]$CM-MgO, which indicated that it contained more micropores than CM-MgO. Both the increase of the total surface area, and the decrease of the average pore diameter also occurred in larger extent in

Table 1. Surface areas and pore characteristics of MgO samples calculated from the isotherms of nitrogen adsorption-desorption

	As prepared (after 1st cycle)						Modified (after 2nd cycle)					
	S_{total} (m^2/g)	$S_{>meso}$[a]	S_{micro}	$\%S_{micro}$	V_{pore} (cc/g)	$r_{average}$ (Å)	S_{total}	$S_{>meso}$	S_{micro}	$\%S_{micro}$	V_{pore}	$r_{average}$
CM-MgO	9.83	7.92	1.91	19.4	0.0233	94.87	23.83	6.97	16.86	70.8	0.0360	60.38
$[Fe_2O_3]$CM-MgO	8.96	6.80	2.16	24.1	0.0261	116.52	41.35	10.79	30.56	73.9	0.0456	44.08

[a] $S_{>meso} = S_{total} - S_{micro} = S_{meso} + S_{macro}$

[Fe_2O_3]CM-MgO than in CM-MgO. In both samples, the micropores contributed more than 70% to the total surface area, which suggested the increase of the total surface area by the second cycle treatment was mostly due to the generation of the micropores. Comparison on the subtracted values (S_{total}-S_{micro}) also indicated that the surface area by mesopore was also increased in [Fe_2O_3]CM-MgO after the second cycle. With the increase, a small step in the hysteresis was shown to develop around relative pressure of 0.47. Even though the size of the hysteresis was small, it's shape was prominent type H3, which was for a slit-shaped pore.[27] The pore size distribution obtained from the isotherm showed that the mesoporous slit had a dimension of around 30 Å. Therefore, not only the micropores, but also slit-type mesopores were generated by the second cycle treatment, and the surface modification occurred in larger extent in [Fe_2O_3] CM-MgO than in CM-MgO. This observation indicated the surface of [Fe_2O_3]CM-MgO was more prone to the chemisorption by water than CM-MgO, which corroborated the FTIR and PXRD observations described above.

Conclusion

It was demonstrated that surface of MgO could easily be modified by cycles of hydration-dehydration, turning its non-porous inert surface into a very porous active one. More than 70% of the surface area was observed to be originated from the micropores which were generated during the cycles. It was shown that the generation of the micropores was closely related to the extent of the bulk hydroxylation. The overlayer of Fe_2O_3 over the MgO in the core/shell type composite metal oxide enhanced the bulk hydroxylation and the generation of the micropores. This enhancement of surface modification by the overlayer of Fe_2O_3 added up one more reason to the ones proposed in previous report to explain why surface reactivity of MgO was greatly increased by putting the overlayer of Fe_2O_3.[18]

Acknowledgment. The support by the Korean Science and Engineering Foundation (961-0306-065-2) is acknowledged with gratitude.

References

1. Gillan, M. J.; Kantorovich, L. N.; Lindan, P. J. D. *Current Opinion in Solid State & Materials Science* **1996**, *1*, 820.
2. Causaà, M.; Dovesi, R.; Pisani, C.; Roetti, C. *Surface Science* **1986**, *175*, 551.
3. Scamehorn, C. A.; Hess, A. C.; McCarthy, M. I. *J. Chem. Phys.* **1993**, *99*, 2786.
4. Pugh, S.; Gillan, M. J. *Surface Science* **1994**, *320*, 331
5. Scamehorn, C. A.; Harrison, N. M.; McCarthy, M. I. *J. Chem. Phys.* **1994**, *101*, 1547.
6. Langel, W. L.; Parrinello, M. *J. Chem. Phys.* **1995**, *103*, 3240.
7. Kantorovich, L. N.; Holender, J. M.; Gillan, M. J. *Surface Science* **1995**, *343*, 221.
8. Nada, R.; Hess, A. C.; Pisani, C. *Surface Science* **1995**, *336*, 353.
9. Coluccia, S.; Tench, A. J.; Segall, R. L. *J. Chem. Soc., Faraday Trans. I* **1979**, *75*, 1769.
10. Urano, T.; Kanaji, T. *Surface Science* **1983**, *134*, 109.
11. Onishi, H.; Egawa, C.; Aruga, T.; Iwasawa, Y. *Surface Science* **1987**, *191*, 479.
12. Lin, S. -T.; Klabunde, K. J. *Langmuir* **1985**, *1*, 600
13. Li, Y. -X.; Klabunde, K. J. *Langmuir* **1991**, *7*, 1388.
14. Li, Y. -X.; Koper, O.; Atteya, M.; Klabunde, K. J. *Chem. Mater.* **1992**, *4*, 323
15. Klabunde, K. J.; Khaleel, A.; Park, D. *High Temp. Mater. Sci.* **1995**, *33*, 99.
16. Stark, J. V.; Park, D. G.; Lagadic, I.; Klabunde, K. J. *Chem. Mater.* **1996**, *8*, 1904.
17. Klabunde, K. J.; Stark, J.; Koper, O.; Mohs, C.; Park, D. G.; Decker, S.; Jiang, Y.; Lagadic, I.; Zhang, D. *J. Phys. Chem.* **1996**, *100*, 12142.
18. Kim, H. J.; Kang, J.; Park, D. G.; Kweon, H. -J.; Klabunde, K. J. *Bull. Korean Chem. Soc.* **1997**, *18*, 831.
19. Carrott, M. R.; Carrott, P.; de Carvalho, M. B. *J. Chem, Soc., Faraday Trans.* **1991**, *87*, 185.
20. Lowell, S.; Shields, J. E. *Powder Surface Area and Porosity 3rd Ed.*; Chapman & Hall: London, UK, 1991; p 11
21. Johnson, M. F. L. *J. Catal.* **1978**, *52*, 425.
22. Itoh, H.; Utamapanya, S.; Stark, J.; Klabunde, K. J., Schlup, J. R. *Chem. Mater.* **1993**, *5*, 71.
23. Carrott, M. R.; Carrott, P.; de Carvalho, M. B.; Sing, K. S. W. *J. Chem, Soc., Faraday Trans.* **1993**, *89*, 579.
24. Green, J. *J. Mater. Sci.* **1983**, *18*, 637.
25. Kim, M. G.; Dahmen, U.; Searcy, A. W. *J. Am. Ceram. Soc.* **1987**, *70*, 146.
26. Beruto, D.; Botter, R., Searcy, A. W. *J. Am. Ceram. Soc.* **1987**, *70*, 155.
27. Gregg, S. J.; Sing, K. S. W. *Adsorption, Surface area and Porosity 2nd Ed.*; Academic press: London, UK, 1982; p 111.